Natural Dye-Sensitized Solar Cell Based on Zinc Oxide

Salah Abdulla Hasoon[1], Raad M.S. Al-Haddad[2], Oras Tariq Shakir[1], Issam M. Ibrahim[2]

Abstract— Thin Film of ZnO nanoparticles paste are spread on transparent conducting ITO coated glass using doctor-blade method, the average particle size of about 16.4nm. Natural dyes extracted from pomegranate and spinach were used as sensitizers to fabricate dye sensitized solar cells (DSSCs). The thin films were studied by absorption spectra of all dyes were performed by UV-Visible spectroscopy which showed that the dye absorbed light in the visible region from (200-325)nm for chlorophyll pigment and (500-530)nm for anthocyanin pigment. The optical band gap was found to be 3.5eV. X-Ray diffraction, Atomic Force Microscopy and Scanning Electron Microscopy were also investigated.

Index Terms— Dye-Sensitized Solar Cell, ZnO, Nanoparticles, UV-Visible Spectroscopy

1 INTRODUCTION

DYE sensitized solar cells are a type of photoelectrochemical cell. One of the main differences between dye-sensitized solar cells and other types of solar cells is the way charges are separated [1].Dye-sensitized solar cells (DSSCs) are promising, relatively low cost, and green energy photovoltaic devices. DSSCs consists of two conducting glass electrode coated with porous nanocrystalline wide-band gap semiconductor oxide film, such as ZnO nanoparticles which have the dye adsorbed onto their surface, whereas the counter electrode, is coated with platinum or graphite, there is an electrolyte solution that contains the redox couple that regenerates the dye [2,3]. The nanostructured oxide films are particularly attractive for DSSCs as they provide a large surface area for dye anchoring. The working principle of a dye-sensitized solar cell is schematized in Figure (1). The device is comprised of two faced electrodes, a photoanode and a counter electrode, with an electrolyte in between. Both electrodes are usually made from a sheet of common float glass coated on one side with a thin transparent conductive layer of indium-doped tin oxide (ITO). Surface electrical resistivity of a few Ohm squares can be easily obtained while preserving a good optical transmission over the whole visible and near infrared spectrum [4]

Thus (DSSCs) have many advantages comparing with the Si based photovoltaics, it is not sensitive to the defects in semiconductors and it is possible to realize the direct energy transfer from photons to chemical energy [5]. The semiconductor substance that forms the core of the photoelectrode (PE) should be chemically stable and inert towards the electrolyte species, it should have a lattice structure suitable for dye bonding, its conduction band should be located slightly below the LUMO level of the dye in order to facilitate efficient electron injection, and it should be available in nanostructure form to increases the effective surface area for dye adsorption approximately by a factor of thousand, improving the sunlight harvesting efficiency [6]. ZnO is a wide-band-gap semiconductor that possesses an energy-band structure and physical properties similar to those of TiO_2 ,but has higher electronic mobility that would be favorable for electron transport, with reduced recombination loss, the direct band gap is (3.37 eV), higher exciton binding energy (60 meV) compared to TiO_2 (4 meV), and higher electron mobility ($200 cm^2V^{-1}s^{-1}$) over TiO_2 ($30 cm^2V^{-1}s^{-1}$). However, the efficiency of the DSSC based on ZnO nanostructures is still very low (5%) when used in DSCs [7- 9]. The dye that is used as a photosensitizer plays a main role in the process of DSSCs. The efficiency of the cell is critically dependent on the absorption spectrum of the dye and the anchor of the dye to the surface of the semiconductor [10, 11]. Anthocyanin dyes are water-soluble and vacuolar pigments that may appear red, purple, or blue depending on the PH. Anthocyanins absorb light in the blue-green region between the 450 and 600 nm wavelengths; this allows many fruits and plants to reflect red, purple, or blue[12].

[1] *Dr. Salah Abdulla Hasoon Solid state physics College of Science for Women physics department-University of Baghdad- Baghdad Iraq .Mobile: +9647801256859, E-mail:salahabd55@yahoo.com*

[2] *Dr. Raad M. S. Al-Haddad Physics of Solid College of Science physics department-University of Baghdad- Baghdad Iraq. Mobile: +9647901270618 E-mail: alhaddadraad@yahoo.com*

[1]*M.Sc Student. Oras Tariq Shakir Solid state physics College of Science for Women physics department -University of Baghdad-Baghdad Iraq. Mobile: +9647903782925, E-mail:orastariq99@yahoo.com*

[2]Dr. *Issam M.Ibrahim* Solid state physics College of Science physics department -University of Baghdad-Baghdad Iraq . *Mobile: +9647702646902*, E-mail: *dr.issamiq@gmail.com*

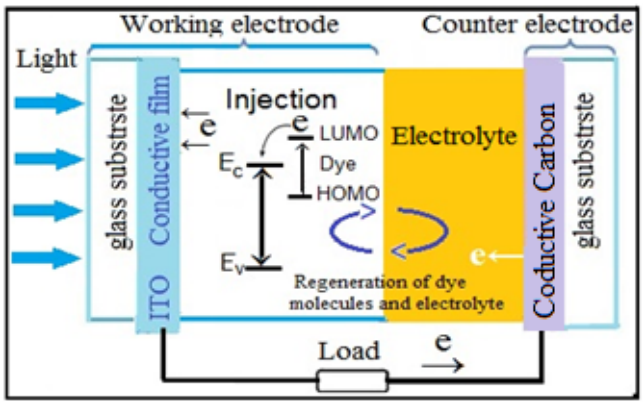

Fig. 1. Shows schematic illustration of operation principle of dye sensitized solar cell [13] .

2 EXPERIMENTAL

2.1 Synthesis of ZnO Nanoparticles

In a typical synthesis, of ZnO nanoparticles is carried out by sol gel process, at (80-90℃). Solution contain 0.2M/l of zinc acetate dihydrate [$(CH_3COO)_2Zn.2H_2O$] was prepared by dissolving (2.195 gm) of zinc acetate dihydrate in (100ml) distilled water/ethanol, and stirred in ambient atmosphere. Potassium hydroxide KOH (1.122 gm) is dissolved in 10ml distilled water and was added to the above solution drop wise under continuous stirring. After few minutes solution turn into jelly form and a milky white solution was obtained, the mixture was refluxed for 3 h at (80-90)℃ without stirring. The resulting suspension was centrifuged to retrieve the product, and the mixture was washed with distilled water in an ultrasonic bathwater and then the powder was dried at 70 ℃ over night.

2.2 Natural Dye Extraction

To extraction the Anthocyanin Pigment from Pomegranate, we bought fresh pomegranate fruit, grabbing the seeds and after removing any white pith from the seeds, we put it in clean mortar to grinding the seeds, we finally got the pomegranate juice and putting it in a clean dish. In the other hand the chlorophylls and the different accessory pigments can be extracted from plants using solvent based methods; Green portion from Spinach leaves was taken out after cleaning the surfaces of leaves with acetone, after that we converted in to paste by grinding Pestle, and 10 ml acetone was added and again grind. A Filter paper was kept over the funnel of beaker and above paste of leaves was poured over the filter paper, and then 30 ml acetone was dropped over the past, and finally, drop by drop chlorophyll of Spinach leaf come out from the funnel and settled in beaker ultimately kept it in clean petri-dish.

2.3 Preparation of dye-sensitized solar cells

ITO conductive glass sheets (Asahi Glass, tin-doped indium oxide, sheet resistance: 15 /Ω²), were first cleaned in a detergent solution ethanol, and then dried. Zinc Oxide Paste were prepared by adding few drops of dilute nitric acid (2.5ml) to ZnO powder and completely mixed with each other by grinding pestle or using a mortar, then we deposited the ZnO paste on the ITO conductive glass by doctor-blading technique in order to obtain a ZnO film with a thickness of 112nm and an area of 1cm². The ZnO films was sintered at 400 ℃ for 30 min and then. After cooling, the ZnO electrode was immersed in a natural dye for 15min for pomegranate juice and over night for spinach extract .The dye-sensitized ZnO electrode and a carbon dust counter electrode was assembled to form a solar cell by sandwiching a redox (I^-/I^{3-}) electrolyte solution.

3 RESULTS AND DISCUSSION

3.1 X-Ray Diffraction Measurement and Morphological Studies

In order to study the structural properties, the crystalline structure was examined by X-ray diffractions using. This system recorded the intensity as a function of Bragg's angle. Crystal structures of films were analyzed by using a (Philips PW) X-ray diffractometer system with CuK_α target, radiation (λ=1.5406Å) with scanning angle: (20- 70°).

The optical Measurement absorbance spectra of the ZnO thin film within the wavelength ranging from (190 - 1100 nm) at room temperature were measured using UV-Visible (SP – 8001 spectrophotometer over (Meterrech)).

The surface morphology and the size of ZnO particles were analyzed using atomic force microscope (AFM), (SPM, Model AA3000), tip NSC35/AIBS from Angstrom Advanced Inc (USA), and Scanning electron microscopy (S-4160 HITACHI) was used to inspect the size and morphology of specimens at very high magnifications. The magnification can go 100 K, and 300 nm Scale. During SEM analysis, a beam of electrons is focused on a spot volume of the specimen. The electron beam has energies that range from a few keV to 20 keV and it is focused by two condenser lenses into a beam with a very fine spot size.

3.2 Structural Properties

XRD pattern of the prepared ZnO film is shown in Fig. 2. It is clear from the figure that all the diffraction peaks are highly crystalline as well as the diffraction peaks are well defined and in accordance with the typical wurtzite hexagonal structure. We have Six major diffraction peaks were seen at 2θ (31.79, 34.44, 36.26, 47.54, 56.61, 62.87) which can be assigned to diffraction from (100), (002), (101), (012), (110), (013), (200), (112) planes respectively, according to the data base in JCPDS card (96-900-4180). This revealed that the resultant nanoparticles were pure ZnO with a hexagonal wurtzite structure (a=3.247Å, c=5.622Å). There is no diffraction peaks corresponding to the impurity could be detected in this pattern, which implies hexagonal phase ZnO nanoparticles. The mean crystalline size was calculated from the full-width at half-maximum (FWHM) of

XRD lines by using the Debye-Scherrer equation (1).

$$D = \frac{K\lambda}{\beta \cos\theta} \qquad (1)$$

Where D is the mean size of crystallites (nm), K is crystallite shape factor a good approximation is 0.9, λ is X-ray wavelength, β is full width at half the maximum (FWHM) in radians of the X-ray diffraction peak and θ is the Bragg angle [14]. It can be seen that the average size of nanoparticles is16.44nm from table (1).

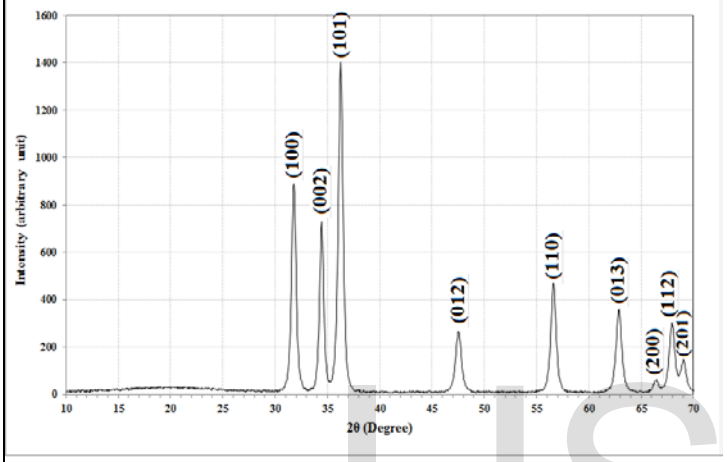

Fig. 2.XRD Spectrum of the Nanocrystalline ZnO Thin Film.

TABLE 1
STRUCTURAL PARAMETERS OF THIN

2θ (Deg.)	FWHM (Deg.)	d_{hkl} Exp.(Å)	G.S (nm)	d_{hkl} Std.(Å)	hkl
31.7913	0.4855	2.8125	17	2.8174	-100
34.4491	0.4414	2.6013	18.9	2.6037	-2
36.2679	0.5029	2.4749	16.6	2.478	-101
47.5417	0.6134	1.911	14.2	1.9122	-12
56.613	0.5626	1.6245	16	1.6266	-110
62.8773	0.5992	1.4768	15.5	1.4778	-13
66.4206	0.5367	1.4064	17.7	1.4087	-200
67.9588	0.601	1.3783	15.9	1.3795	-112
69.0584	0.5953	1.359	16.2	1.3598	-201

3.3 Atomic Force Microscope (AFM)

Atomic force microscope (AFM) is a high resolution scanning probe microscopy. It is a useful tool used by the research community in material science to investigate the surface profiles in three dimensions at the nanoscale level and it is also used in manipulating atoms. Figures 3A and 3B illustrates two and three dimensional AFM images (2 μm × 2μm) of the ZnO paste were deposited by using doctor-blade method. It is clear, the average diameter 65.70nm with roughness 0.353nm, this means that the producers from ZnO particles within the range of nanoscale.

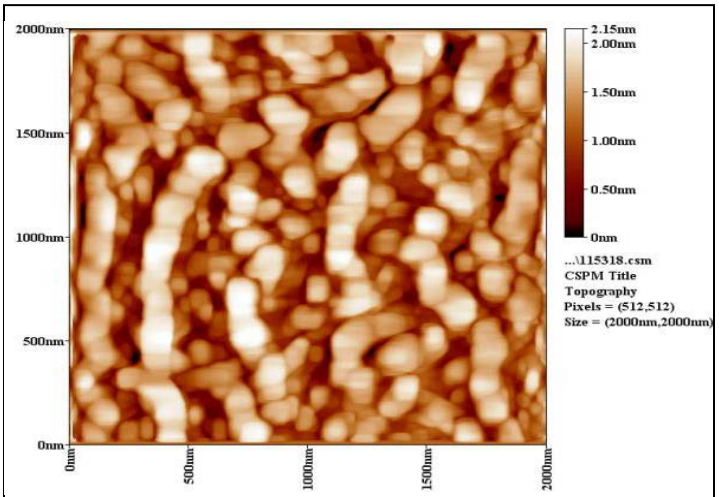

Fig. 3A .shows the 2D, 3D surface plot AFM picture of the nanocrystalline ZnO film.

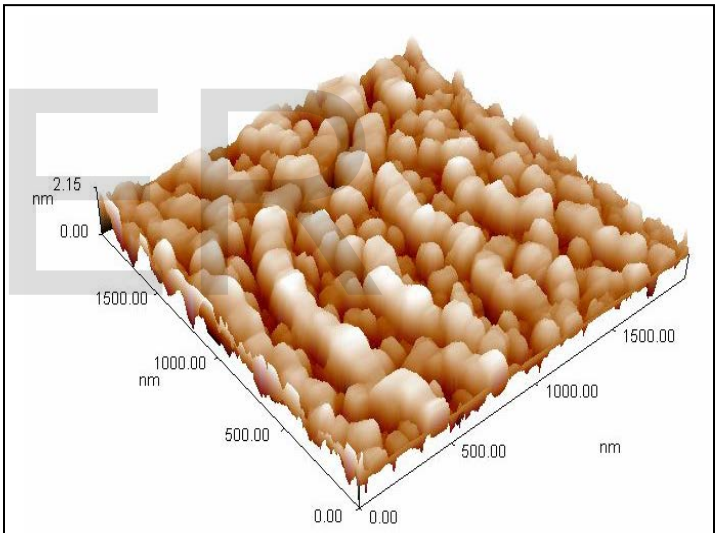

Fig. 3B .shows the 3D surface plot AFM picture of the nanocrystalline ZnO film.

3.4 Scanning Electron Microscope (SEM) of ZnO Film

The key points for DSSC application is surface morphology. Thus it is significant to study the Surface morphology of the ZnO film.

An SEM micrograph was used to examine the topography and morphology of the samples. It provides essential information about shape, size, and the growth mechanism of the ZnO nanoparticles. Figure (4) shows the low and high magnification SEM images of the sample grown on the glass substrate. The figure clearly indicates the morphology of the particles to be roughly spherical, non-homogeneous. Some of the particles are agglomerates with an average grain size of approximately (50.62) nm, this consequence almost similar to

AFM measurement.

However, it was observed that there was a difference between the size measurement using XRD and SEM. The reason is well known. In SEM, the grain size was measured by the differences between the visible grains boundaries while in, the XRD method, the measurement was confined to the crystalline region that diffracted x-ray coherently. This was a more stringent criterion and led to smaller grain size.

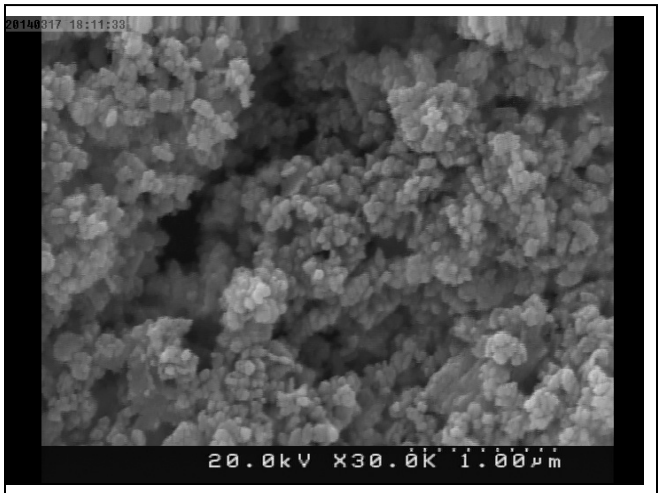

Fig. 4A. shows SEM images of the ZNO film, at low magnification.

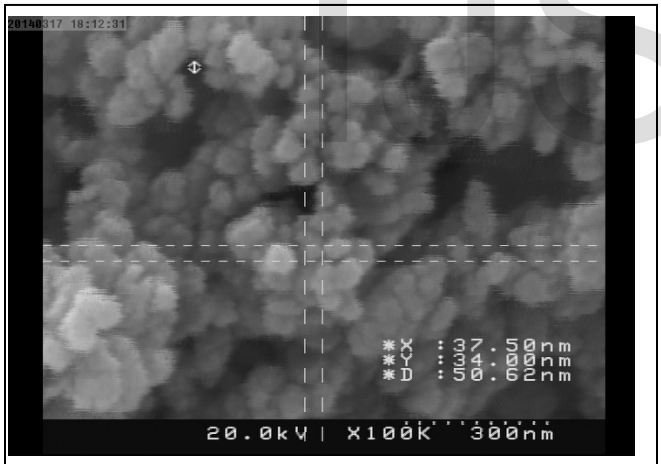

Fig. 4B. shows SEM images of the ZNO film, at high magnification.

4 Optical Characterizations

4.1 Optical Energy Gap (E^0_g) For ZnO Films

The absorption spectrum of ZnO nanopowder (colloidal nanoparticles) is shown in Figure (5), the sample show strong UV absorption in visible region with peak maximum at 357nm indicating band- to-band excitation of ZnO, which is used for calculation of optical band gap of nanoparticle by using equation (2).[15]

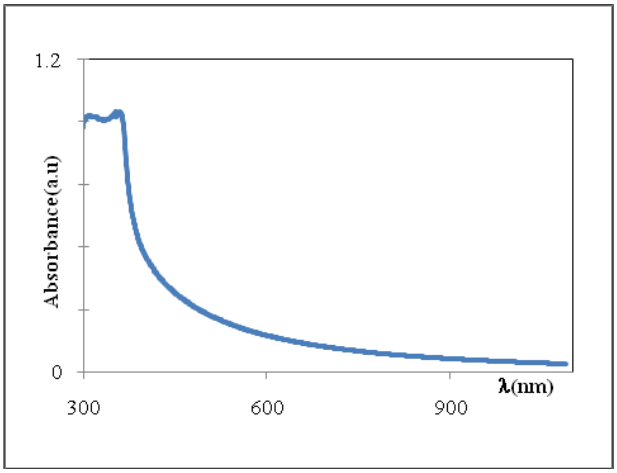

Fig. 5. shows the optical absorbance spectra of ZnO powders prepared from 0.2M Zinc acetate.

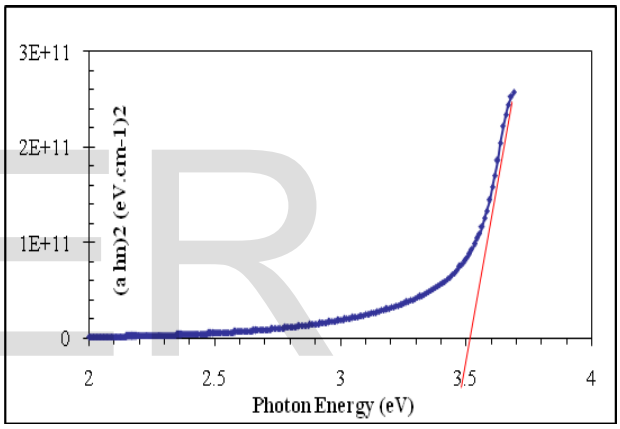

Fig. 6. Evolution of the $(\alpha h\upsilon)^2$ vs. $h\upsilon$ curves of ZnO thin film prepared from (0.2M) Zinc acetate.

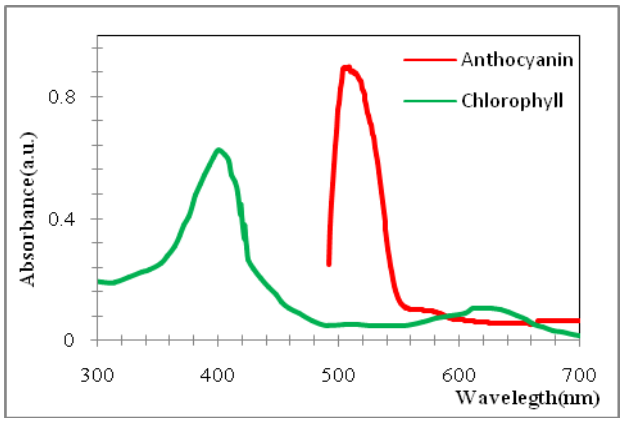

Fig. 7. Shows the absorption spectra of chlorophyll and anthocyanin pigment .

$$\lambda(nm) = \frac{1240}{E_g(ev)} \qquad (2)$$

The optical absorption provides the dependence of the absorption coefficient (α) on the photon energy ($h\nu$) for direct allowed [16]

$$(\alpha h\nu) = (h\upsilon - E_g)^{\frac{1}{2}} \qquad (3)$$

we applied Tauc plot to find the optical band gap by plotting $(\alpha h\nu)^2$ vs photon energy using the data obtained from optical absorption spectra and extra plotted to $\alpha = 0$ as shown in figure (6) . The optical band gap determined from this curve is ~3.5eV.

4.2 UV-Visible Spectroscopy for the Dye

The absorption spectra of chlorophyll and anthocyanin pigment are shown in figure (7), the absorption spectra showed the presence of distinct absorption peaks in the visible region at about 400 nm and a small peak at about 617 nm for the extract of chlorophyll Huizhi Zhou et al. [17]. The absorption spectra showed also the presence of peak at (503-510 nm) for anthocyanin pigment dye [18]. Results show that the absorption intensity of anthocyanin dye is highest that than chlorophyll, it can be seen the absorption of two dyes in the visible region (approximately 400 - 620 nm). This proves the possibility used as sensitizers to fabricate dye-sensitized solar cells (DSSCs) as mentioned by Chang et al. [19].

4.3 Photovoltaic Properties

Photovoltaic tests of the fabricated DSSCs using these natural dyes as sensitizers were performed by measuring the I–V curve of each cell under irradiation with white light (100 mW/cm²) from xenon arc lamp and at room temperature(22.3℃) with cell area 1cm².. The values of fill factor (FF) was calculated by applying the following generalized equat

$$FF = \frac{P_{max}}{I_{sc}\,.\,V_{0c}} \qquad (4)$$

Where V_{0c} and I_{sc} are respectively the open circuit voltage and short circuit current. P_{max} is the maximum power delivering point. The I-V characteristics of the prepared DSSCs taking pomegranate juice, chlorophyll extract from spinach as the natural dye by using Doctor-blade with ZnO nanoparticles is shown in figure (8). The photoelectric conversion efficiency (η) of DSSC is given as

$$\eta = \frac{I_{sc}\,.V_{oc}}{P_{in}}\,.FF \qquad (5)$$

Where P_{in} is the incident light power. Table (2) shows the data acquired from measuring the photoelectric conversion efficiency of the DSSCs

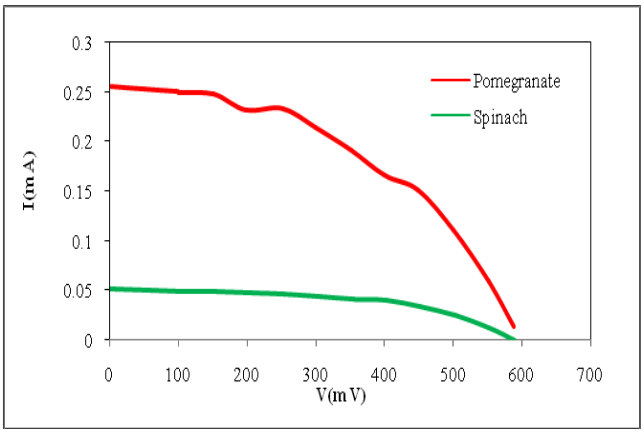

Fig. 8. Photocurrent voltage characteristics spinach and pomegranate dye.

TABLE 2
PHOTOELECTROCHEMICAL PARAMETERS OF THE DSSCs SENSITIZE BY VARIOUS NATURAL DYES

Natural dye pigment	Imax (mA)	Vmax (mV)	Isc (mA)	Voc (mV)	FF%	η%
pomegrante juice(anthocyanin)	0.15	450	0.255	600	0.44	0.07
spinach chlorophyll	0.04	410	0.052	590	0.53	0.0164

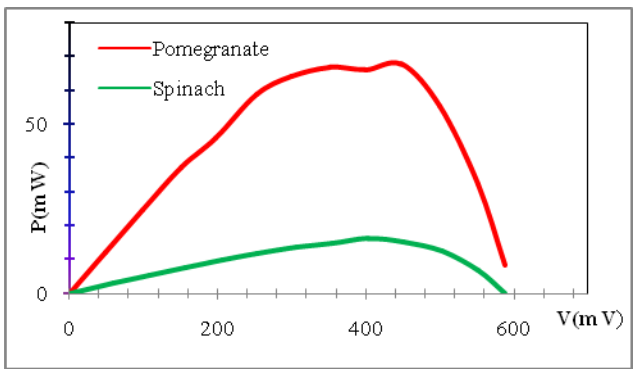

Fig. 9. Shows the power-voltage characteristics curves of the DSSCs sensitized by: spinach and pomegranate using Doctor-blade method..

The DSSC output power was calculated using the I-V data. Figure (9) shows the power as a function of V for the DSSC sensitized by spinach and pomegranate juice.

The lowest P_{max} value come from the DSSC sensitized with spinach which may be assign to weak bonding between the dye molecule and ZnO particles. good electric conversion ability in a DSSC is highly dependent on disponible bonds between the dye molecules and ZnO particles, in which electrons can transport from excited dye molecules to ZnO, chlorophyll dye is lower than anthocyanin dye, therefore, this is Compatible with the results of Chang et al.[10, 19].

Some research workers have found that the energy conversion efficiency was 0.0277%. with anthocyanin dye Extracted from strawberry [20] However, our results were 2.5 times higher than in others, this may have influenced the results of the experiment since plants contain different components which equally produce different results [20].

5 CONCLUSIONS

Hexagonal ZnO nanopartical were synthesis successfully without using any capping agent through sol gel process at 80-90^0 C. we were also able to make dye-sensitized ZnO solar cells by using natural dye (pomegranate, chlorophyll) by using an electrolyte with a KI_3 redox couple and a carbon dust counter-electrode. Natural dyes as alternative sensitizers for DSSCs are expected to be promising because of many reasons such as the simple preparation technique and low cost. The Preparation and characterization of ZnO nanoparticles using XRD, AFM and SEM, are presented in this work. The SEM picture of the ZnO film shows that the nanoparticles are non-homogeneous and has a porous agglomerate structure consisting mainly of spherical crystalline particles with about 50.62nm diameter.

ACKNOWLEDGMENT

The authors wish to thank College of Science and college of Science for women /Department of Physics /University of Baghdad to allow us for providing Instrumental and laboratory facilities to carry out this work

REFERENCES

[1] B. E. Hardin, H. J. Snaith and M. D. McGehee. " The renaissance of dye-sensitized solar cells," *Nature photonics*, vol. 6, pp. 162-169, 2012.

[2] T.M. El-Agez, A.A. El Tayyan, A. Al-Kahlout, S.A. Taya, and M.S. Abdel-Latif. " Dye-Sensitized Solar Cells Based on ZnO Films and Natural Dyes," *International Journal of Materials and Chemistry*, vol.2, no.3, pp.105-110, 2012.

[3] J. Wu, Z. LAN, S. Hao, P. Li, J. Lin, M. Huang, L. Fang, and Y. Huang,"Progress on the electrolytes for dye-sensitized solar cells," *Pure Appl. Chem.,* vol. 80, no. 11, pp.2241–2258, 2008.

[4] M. Graetzel." Solar Energy Conversion by Dye-Sensitized Photovoltaic Cells, Inorg.Chem" vol.44, no.20, pp. 6841-6851.2005.

[5] D. Wei. " Dye Sensitized Solar Cells," *Int. J. Mol. Sci*., vol.11, pp. 1103-1113. 2010.

[6] M. Gratzel. " Conversion of sunlight to electric power by nanocrystalline dyesensitized solar cells," *Journal of Photochemistry and Photobiology: Chemistry*. vol. 164, no. 1-3, pp. 3-14, 2004.

[7] Q. Q. Zhang, C.S. Dandeneau, X. Zhou, and G.Cao, "ZnO Nanostructures for Dye-Sensitized Solar Cells, ". *Adv. Mater*., vol. 21, pp.4087–4108, 2009.

[8] J. Han, F. Fan, C. Xu , S. Lin., M. Wei, X. Duan and Z.L. Wang," ZnO nanotube-based dye-sensitized solar cell and its application in self-powered devices," *Nanotechnology*, vol. 21, no.1,7, 2010.

[9] M. K. Erhaima, R. A.AL-ansari, N. F.Habubi," Structural and Optical Properties of Cobalt-Doped Zinc Oxide Thin Films Prepared By Spray Pyrolysis Technique," *Baghdad Science Journal*, vol.7, no. 1, pp, 69-75, 2010.

[10] H. Chen, Z. Duan, Y.G. Lu, A. D. Pasquier, " Dye-sensitized solar cells combining ZnO nanotip arrays and nonliquid gel electrolytes, " Minerals Metals & Materials Society, *Journal of Electronic Materials*, vol. 38, no. 8, pp. 1612-1617, 2009.

[11] T. M. El-Agez, A. A. El Tayyan, A. Al-Kahlout, S. A. Taya, M. S. Abdel-Latif, " Dye-Sensitized Solar Cells Based on ZnO Films and Natural Dyes, ". *International Journal of Materials and Chemistry*. vol. 2, no. 3, pp. 105-110, 2012.

[12] M.N. Merzlyak, O. B. Chivkunova, A. E. Solovchenko and K. R. Naqvi, " Light absorption by anthocyanins in juvenile, stressed, and senescing leaves, ". *Journal of Experimental Botany*., vol. 59, no. 14, pp. 3903-391, 2008.

[13] Q. Zhang, G. Cao," Nanostructured photoelectrodes for dye-sensitized solar cells," Nano *Today*., vol. 6, pp. 91—109, 2011.

[14] A. Monshi, M.R. Foroughi, and M.R. Monshi," Modified Scherrer Equation to Estimate More Accurately Nano-Crystallite Size Using XRD," *World Journal of Nano Science and Engineering*, vol. 2, pp. 154-160, 2012.

[15] M. K. Patra, K. Manzoor, M. Manoth, V. S. Choudhry, S. R. Vadera, N. Kumar," Optically transparent colloidal suspensions of single crystalline ZnO quantum dots prepared by simple wet-chemistry," Journal *of Optoelectronics and advanced materials*, vol. 10, no. 10, pp. 2588 – 2591 2008.

[16] R. S. Mane, W. J. Lee, H.M. Pathan, and S. H. Han, "Nanocrystalline TiO2/ZnO thin films Fabrication and application to dye-sensitized solar cells, " *The Journal of Physical Chemistry B*., vol. 109, no. 51, pp. 24254–24259, 2005.

[17] H. Zhou, L. Wu, Y. Gao, and T. Ma, " Dye-sensitized solar cells using 20 natural dyes as sensitizers, " *Journal of Photochemistry and Photobiology A: Chemistry*., vol. 219, pp. 188–194. 2011.

[18] S. M. Milenkovic, J. B. Zvezdanovic, T. D. Andelkovic, and D. Z. Markovic," The identification of chlorophyll and its derivatives in the pigment mixtures: HPLC-chromatography, visible and mass spectroscopy studies," *Advanced technologies*, vol. 1, no.1, pp. 16-24, 2012.

[19] Ho. Chang, M. J. Kao, T. L. Chen, H. G. Kuo, K. C. Choand, and X. P. Lin, " Natural Sensitizer for Dye-Sensitized Solar Cells Using Three Layers of Photoelectrode Thin Films with a Schottky Barrier, " *Am. J. Engg. & Applied Sci*., vol. 4, no. 2, pp. 214-222, 2011.

[20] J. Etula,"Comparison of three Finnish berries as sensitizers in a dye-sensitized solar cell," *European Journal for young scientists and Engineers*, vol.1, pp. 5-23, 2012.